# European Research Infrastructure supporting Smart Grid Systems Technology Development, Validation and Roll Out

Technical Report TA User Project

# CHROME

| | |
|---|---|
| Grant Agreement No: | **654113** |
| Funding Instrument: | **Research and Innovation Actions (RIA) – Integrating Activity (IA)** |
| Funded under: | **INFRAIA-1-2014/2015: Integrating and opening existing national and regional research infrastructures of European interest** |
| Starting date of project: | **01.11.2015** |
| Project Duration: | **54 month** |

| | |
|---|---|
| Contractual delivery date: | **25-05-2018** |
| Actual delivery date: | **09-05-2018** |
| Name of lead beneficiary for this deliverable: | **Tuomas Messo, Tampere University of Technology, Finland** |
| Deliverable Type: | **Report (R)** |
| Security Class: | **Public (PU)** |
| Revision / Status: | **approved** |

*Project co-funded by the European Commission within the H2020 Programme (2014-2020)*

## Document Information

| | |
|---|---|
| Document Version: | 1 |
| Revision / Status: | draft |
| **All Authors/Partners** | Tuomas Messo / Tomi Roinila / Roni Luhtala / Yin Sun / Erik de Jong |
| **Distribution List** | Public |

## Document History

| Revision | Content / Changes | Resp. Partner | Date |
|---|---|---|---|
| 0.1 | Document initiation and basic information added | DNVGL | 16.04.18 |
| 0.9 | Document finalised and submitted for review | Tampere University | 06.05.18 |
| 1.0 | Report completed | Tampere University | 09.05.18 |

## Document Approval

| Final Approval | Name | Resp. Partner | Date |
|---|---|---|---|
| User Group Leader | Tuomas Messo | Tampere University | 09.05.18 |
| Host Technical Team Member | Yin Sun | DNVGL | 09.05.18 |
| Host Leader | Erik de Jong | DNVGL | 09.05.18 |

## Disclaimer



## Copyright Notice

## Table of contents

## Abbreviations

| | |
|---|---|
| *DER* | Distributed Energy Resource |
| *TA* | Trans-national Access |
| *PRBS* | *Pseudo-Random Binary Sequence* |
| *MLBS* | *Maximum-Length Binary Sequence* |
| *FRA* | *Frequency-Response Analyzer* |
| *SNR* | *Signal-to-Noise Ratio* |

## Executive Summary

Grid impedance and the output impedance of grid-connected inverter are important parameters for the operation of grid-connected systems, such as solar, wind, and other distributed-generation systems. The impedance mismatch between the grid and the power converter can generate harmonic resonances, which can cause damage to devices, blackouts and safety hazards. The harmonic resonance may appear to be a power quality problem, but it is actually an indication of lack of system stability margin and may lead to instability and disruption of inverter operation if the grid impedance or the inverter power level further increase. Therefore, accurate grid- and inverter-impedance information is essential for stability assessment and for maintaining stability in future power grids. Since the dynamics of grid-connected systems vary over time and with many parameters, real-time analysis is most desirable.

Our collaborative research project, funded by the Academy of Finland, aims to develop an online impedance-measurement technology to enable real-time stability characterization and adaptive control of grid-connected systems to mitigate the observed harmonic resonance phenomenon. Based on current understanding of the problem, the key to success lies in the availability of accurate harmonic impedance models in stability analysis and careful design of power converters. The proposed technology makes it possible to verify and evaluate the harmonic impedance models at both sub and super-synchronous frequencies from grid-connected systems. The technology can be further used to implement adaptive-control to high-power converters to enhance plug-and-play functionality of grid-connected power converters.

During the first part of the research visit, a measurement setup was implemented which allow extracting the vital impedance characteristics from a three-phase power converter. In the setup, a small-amplitude wideband perturbation is injected to the system, and Fourier analysis is applied to extract the harmonic impedance. The measurement setup can be further used for validation of the harmonic impedance models developed by several different research groups and for certification of power converters in the near future. Impedance measurement at high power level has not been previously reported. However, due to fundamental differences, such as different switching frequency, control bandwidth and parasitic losses, between medium and high–power converters, results from low-power converters are not valid at higher power levels.

During this visit, several impedance measurement methods were tested at a power level of roughly 25 kW. One voltage amplifier was configured to emulate the output impedance of a three-phase converter while another amplifier was used to generate the required small-signal excitation. The effect of the control functions to converter impedance was achieved by using a real-time simulator. The tested algorithms proved to be fast and effective methods to extract the converter impedance online at its nominal operating point. Now that the algorithms have been validated the next visit planned toward the end of year 2018 (or beginning of 2019) will concentrate on measuring impedance with significantly higher power level.

# 1 General Information of the User Project

| | |
|---|---|
| User Project acronym | CHROME |
| User Project title | Converter Harmonic Model Measurement |
| Name of the ACCESS PROVIDER | DNVGL Netherlands B.V. |
| INSTALLATION name | Flex Power Grid Lab |
| Name of the ACCESS PROVIDER representative | Erik de Jong |
| Name of the User Group Leader | Tuomas Messo |
| User Group | 1) Tomi Roinila<br>2) Roni Luhtala |
| Home Institution of the User Group Leader: | Tampere University of Technology |
| Access period | 16.04.2018 – 26.04.2018 |
| Nº of Access Days | 5 |

## 2 Research Motivation

The amount of power electronic converters in power systems is experiencing a growth as never experienced before. Modern power systems may even be solely based on power converters, such as renewable energy –based microgrids, and power systems of all-electric aircraft. The analysis of such systems is more complex than the conventional power systems where power flow is typically from a significant electrical source to distributed loads. There is significant amount of evidence that the analysis (especially stability analysis) of modern AC power systems should be carried out taking into account a wide range of frequencies. Resonance problems have been reported at several kilohertz in offshore wind power plants, grid-connected photovoltaic power plants and data centers. This is an alarming observation, since the penetration of power electronics is bound to keep increasing. Small-signal impedance-based analysis is one of the proposed methods to identify and mitigate the resonance problems. The main benefit of impedance-based analysis is the fact that online measurements can be used instead of models, which are always approximations and may even be impossible to derive due to high complexity of power-electronics based power systems.

### 2.1 Objectives

The main long-term objective of this project is to successfully prototype a method to measure small-signal impedance from a power converter operating at or near the power level of 1 MW. The first step is to measure impedance at the power level of roughly 1 MW which allows impedance characterization of most photovoltaic central inverters. Subsequently, the necessary modifications can be done in the future to enable impedance measurement at 8 MW to allow impedance characterization of full power wind power converters (after the visit by DNV-GL or during another visit). Measuring the impedance at the nominal power is important since operating point has a major effect on converter impedance and, thus, its stability in a power system.

The impedance measurement is based on wideband-identification technique. In the method, a broadband excitation such as pseudo-random binary sequence (PRBS) is injected on top of the grid voltages seen by the power converter. The resulting grid voltages and currents are measured, and Fourier techniques are applied to extract the frequency components in both the voltages and currents. The PRBS has been proven to be one of the most promising online methods to obtain impedance information from grid-connected systems. The PRBS is a deterministic and periodic signal. Therefore, the effect of external noise can be computationally reduced, and multiple periods can be applied through spectral averaging to further increase the signal-to-noise ratio (SNR). As a result, the injection amplitude can be kept very small such that normal system operation is guaranteed during the identification. The small injection amplitude is critical when working with such a high power levels not to cause malfunctioning or to trip any of the protection circuits.

In previous research the impedance of low-power converters has been measured by using a three-phase linear amplifier to emulate the behavior of real power system, i.e., the power converter feeds power to the amplifier according to Fig. 2.1. This type of measurement relies on “voltage-type” injection where the PRBS-signal is added on top of the emulated grid voltages ($v_{grid}$).

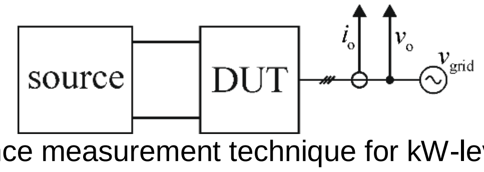


Figure 2.1: Impedance measurement technique for kW-level power converters.

However, in the case of high-power converters, using such a setup is not feasible or realistic, since the linear amplifier should be able to dissipate all the power generated by the converter. The impedance measurement technique requires the output currents or voltages of the power converters ($i_o$ and $v_o$) to be perturbed by an external source or converter. The impedance can be measured from high-power converter by using the “current-type” injection as illustrated in Fig. 2.2. The linear amplifier is configured to inject the perturbation in the current between a back-to-back converter and the power converter from which the impedance is measured ($i_{inj}$). The back-to-back converter (or grid emulator) allows keeping the “grid” frequency and amplitude constant during the measurement to avoid errors due to shifting operating point.

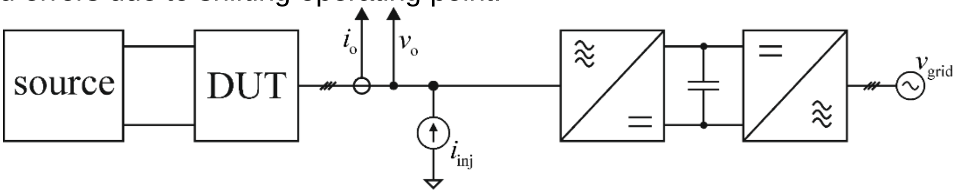


Figure 2.2: Proposed impedance measurement technique for MW-level power converters.

The measurement setup will be first demonstrated by using a power-level of less than 100 kW as illustrated in Fig. 2.3. The laboratory is equipped with a linear power amplifier rated 200 kW. Part of the power supply (100 kW) will be configured to act as the injection amplifier while a second part (100 kW) will act as the device-under-test, from which the impedance is measured. The three-phase grid is reproduced by using the on-site grid emulator.

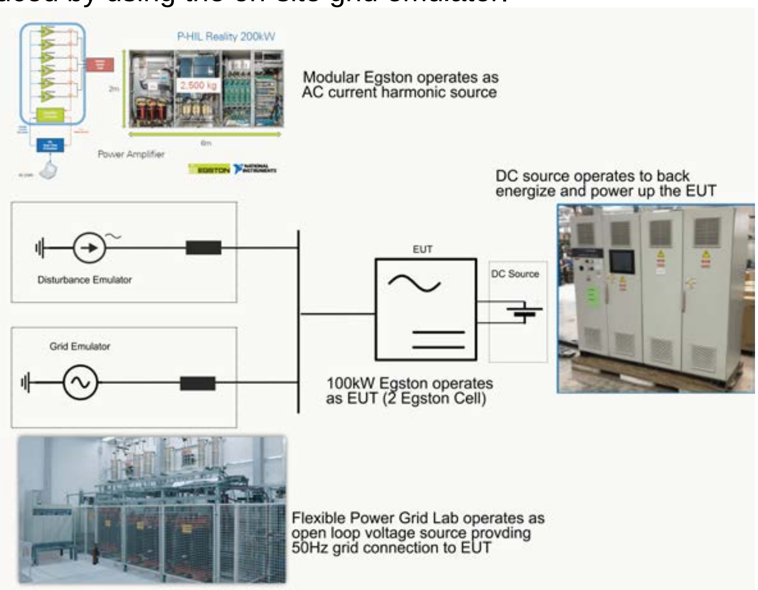


Figure 2.3: Setup for prototyping impedance measurement at 100 kW power-level.

The second demonstration is done at the MW power-level, according to Fig. 2.4. The high-power AC grid emulator acts as the device-under-test while the actual three-phase grid is used as the load. The reason for having different steps is to have the possibility to identify risks and challenges related to the hardware and safety, before the final impedance measurement will be implemented. The proposed plan does not depend on the availability of commercial MW-level power converter during the research visit. Therefore, the measurement method can be demonstrated by using the equipment that already exist in the laboratory.

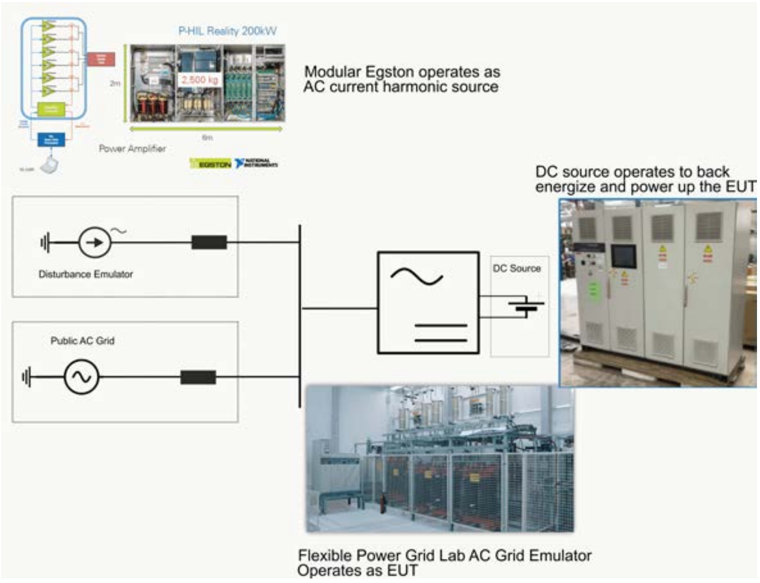


Figure 2.4: Setup for prototyping impedance measurement at MW power-level.

*Harmonic model verification*

The secondary objective is to verify the accuracy of harmonic impedance models developed for high-power wind and solar power converters. Accurate impedance models enable more realistic offline stability studies of modern power systems which experience large penetration of renewable energy source, such as large scale photovoltaic generation or offshore wind power parks. This objective requires successful implementation of the impedance measurement setup.

*Methods for for multiple-input-multiple-output measurements*

Three-phase grid-connected systems are multiple-input multiple-output (MIMO) systems. They have more than one input and output which are typically coupled. In principle, describing a three-phase impedance fully requires at least two measurements to be carried out. All the impedances can be measured by applying a broadband excitation to each input and measuring responses at all outputs in turn, and cross-correlating each input and output signal combination. A good example of such a procedure is the impedance measurement in the direct-quadrature (dq) reference frame.

Applying multiple-input-multiple-output (MIMO) techniques, different coupled components (e.g. d and q components) of the inverter output impedance or grid impedance can be simultaneously measured during a single measurement cycle. Therefore, the operating conditions of the system can be kept constant during the measurements, and the overall measurement time is significantly reduced. One of the objectives of this project is to implement MIMO measurements by using orthogonal pseudo-random sequences. In the method, several perturbations are applied at the same time. Due to orthogonality, the injected energy lies at different frequencies for different injections, and hence, the cross coupling between components is avoided. Consequently, only one measurement cycle is required to obtain all impedances. Therefore, the overall measurement time is drastically reduced. Furthermore, the method guarantees that the system dynamics do not change between the measurements, and hence, the computed bus impedance is not distorted.

## 2.2 Scope

The scope of this research includes methods to enable impedance measurement at high power levels. The impedance measurement is done for a single converter. Different excitation and impedance computation methods are tried and compared.

## 3 State-of-the-Art

Unstable harmonic resonance phenomenon has been recently reported in wind and photovoltaic power plants [1,2]. Similar instability has caused severe problems previously in railway power systems, leading to standardization of impedance characteristics of related power electronic equipment [3]. Extensive work has been done to characterize and prevent similar incidents in power systems with large penetration of renewable energy sources [4-6]. Figure 3.1 illustrates a harmonic resonance appearing in a photovoltaic power plant [1]. The resonance can appear in the sub-synchronous range (below fundamental) or at super-synchronous range (up to several kilohertz).

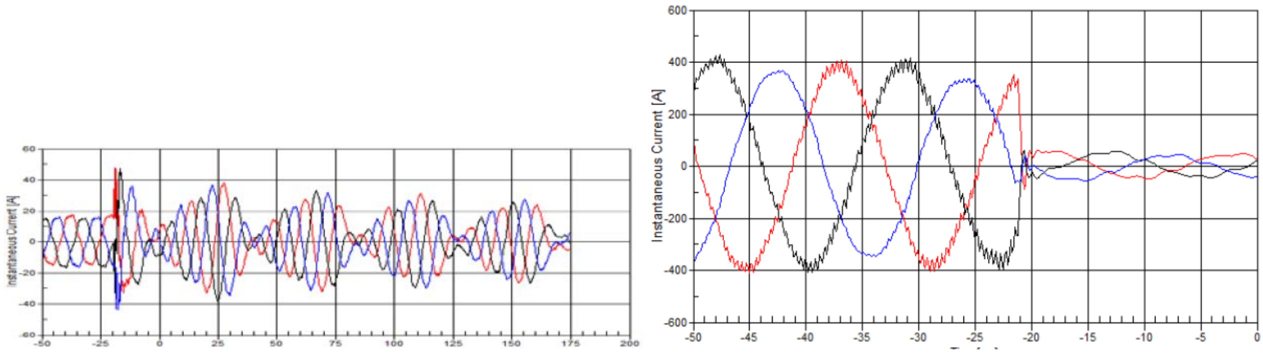


a) b)

Figure 3.1: Harmonic resonance in a grid-connected photovoltaic power plant: a) sub-synchronous and b) super-synchronous resonance [1].

Based on current understanding, the resonance phenomenon can be prevented by careful design of power converter's output impedance [7]. The impedance can be shaped by appropriate selection of internal control parameters of the inverter [8]. The idea is similar to adding a damping resistor to an electrical oscillator. However, in the case of power converter damping is introduced by the converter's digital control system. The impedance can in fact be shaped by trial-and-error method by first measuring the converter impedance in the nominal operating point and subsequently making adjustments to inverter control parameters, until sufficient characteristics are reached. Moreover, the impedance measurement can be used for certification purposes in future, like in the case of railway power systems. Some form of standardization of power converter impedance is likely to happen in near future as EU struggles to increase the share of renewable energy sources [9].

The converter impedance can also be re-designed by using an accurate harmonic impedance model [10]. This approach avoids the time-consuming repeated impedance measurements. However, the impedance model should be verified based on impedance extracted from a real power converter in its nominal operating point. Real power converters suffer from a set of non-idealities that are unknown or not easily re-produced by simulators, delays and nonlinearities. Fig. 3.2 shows the impedance measured from a 10 kW power converter and the corresponding impedance model, which has been obtained at our university's power electronics laboratory previously. The model shows almost perfect match with the measured impedance. Thus, the developed impedance model can be used in stability analysis of power systems with high confidence.

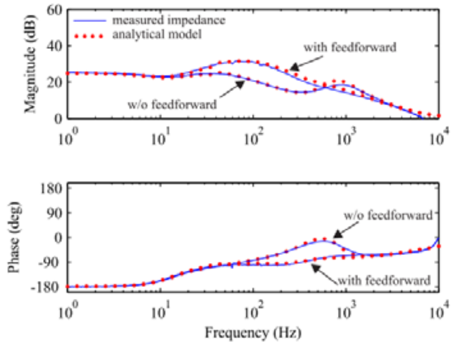


Figure 3.2: Measured impedance and the result from impedance model.

This project aims to develop an impedance measurement setup, which can be used to measure impedance from megawatt-level power converters. The measured impedances can be then used for validating the harmonic impedance models. We have strong experience in measuring impedances in the kilowatt-range [11,12]. However, accurate impedance measurement in megawatt-level requires different considerations because scaling of power levels does not provide correct results. This is due to the fact that component sizing, switching frequency, control bandwidths and parasitics are totally different between kW and MW-level converters.

Impedance measurement from medium-voltage ship power system has been demonstrated in [13]. However, the frequency range is only up to 1 kHz, whereas wind and solar power systems have been reported to suffer from resonances ranging from few hertz up to several kilohertz. Moreover, some control actions, such as active damping, may affect the impedance at frequencies significantly higher than one kilohertz [10].

The research represents the state-of-the-art in the field of online impedance measurement, stability analysis and adaptive control of power-distribution systems. The research has successfully combined expert knowledge from several fields including system identification, small-signal analysis, control theory and power electronics. To date, the methods for online methods in power electronics have been limited by the lack of knowledge of the techniques applied in other fields. Combining and customizing the methods from several scientific fields have made it possible to develop completely new and efficient techniques to improve the operation of power-distribution systems.

# 4 Executed Tests and Experiments

During the access days different impedance measurement methods were prototyped in the FPG Lab. It was decided to use one of the amplifiers to emulate inverter impedance and measure that instead. The solution allows testing of impedance measurement algorithms but also provides better safety, since the amplifiers can limit overcurrents and voltages. Therefore, the risks for equipment damage was reduced significantly.

## 4.1 Test Plan

During the first days the dynamics of amplifiers were measured using a frequency response analyser, to allow designing the outer control loops for the amplifier. Once the outer loops were designed, the stability of the amplifier was validated. Finally the output impedance of the amplifier was measured and the effects of control loops on impedance behaviour were verified. The detailed day-by-day test plan is given below.

16.4.2018, Day 1: TUT researchers familiarize with laboratory staff, common practices and safety regulations.

17.4.2018, Day 2 (access day): Connections and the final layout of the experiment are decided and final simulations are done.

18.4.2018, Day 3 (access day): Experimental test signals are run on HIL-platform with all power outputs offline. The test signal is loaded in the memory of the HIL-simulator to enable perturbing the AC voltage and current in the system.

19.4.2018, Day 4 (access day): The setup is powered on with the intended configuration and without the experimental test signals (or they equal DC 0 volts). The setup is operated at the intended power level.

20.4.2018, Day 5: Reserved for simulation, debugging and re-design of test signals.

23.4.2018, Day 6 (access day): First attempt to measure impedance is made. The setup is powered on with low power level and impedance measurement is carried out. The test signal is injected into the system and currents and voltages are recorded for further analysis.

24.4.2018, Day 7: Reserved for simulation, debugging and re-design of test signals. Attempt is made to identify the impedance based on the measured data from Day 6.

25.4.2018, Day 8 (access day): Second attempt to measure impedance is made. The power level may be higher if no problems or safety issues have been detected during Day 6.

26.4.2018, Day 9: Attempt is made to identify the impedance based on the measured data from Day 8. Recap with DNV-GL personnel.

27.4.2018, Day 10: Reserved for writing final report and planning the content of following visits and collaboration.

## 4.2 Standards, Procedures, and Methodology

Not applicable.

## 4.3 Test Set-up(s)

### 4.3.1 Amplifier Frequency Response

The first test setup included one three-phase amplifier configured to for voltage-mode operation. The amplifier was loaded by another three-phase amplifier to have a better understanding how the amplifier works under loaded condition. The second amplifier was configured for current-mode operation. The purpose of the first experiment was to measure the bandwidth of the voltage amplifier using a frequency response analyser (FRA). The simplified schematics in Fig. 4.1 show the principle of the measurement. A perturbation is made (in dq-domain) to the reference of the voltage amplifier. The reference value and the actual measured voltage is fed back to the FRA, which generates automatically the sine-sweep and computes the frequency response.

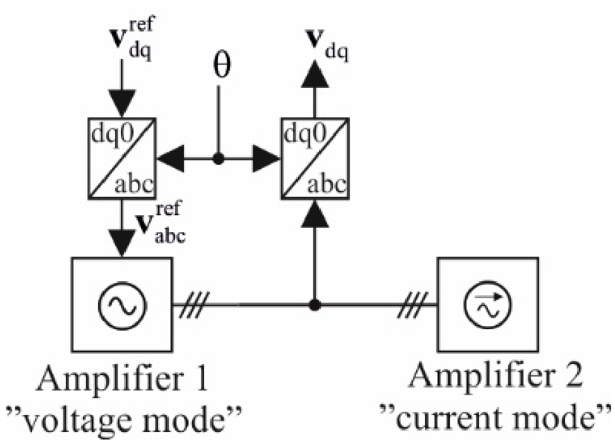


Figure 4.1: Test setup to measure amplifier frequency response.

The measured frequency responses are shown in Fig. 4.2. The direct frequency responses from the reference values to actual measured values are the most important characteristics. The solid blue line depicts the frequency response from reference value of the voltage d-component to the actual measured voltage d-component at the output terminals of the amplifier. The solid red curve represents the same characteristics for the q-components. The magnitude stays within +/- 1.5 decibels at frequencies below 2.5 kHz, which is half of the value given by manufacturer. However, it is not evident if the initial tests by manufacturer had been done under loaded or un-loaded condition. It can be concluded that the bandwidth of the amplifier should be high enough to allow high-bandwidth injection of MLBS signals and to emulate inverter impedance. The cross-channel frequency responses (from d to q and vice versa) have very low magnitude, approximately -30 to -20 decibels indicating that there is no need for special arrangements, such as decoupling networks.

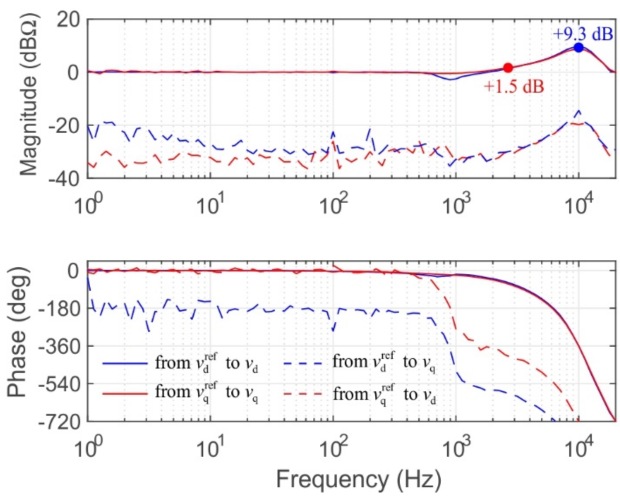


Figure 4.2: Measured frequency responses of the voltage amplifier in the dq-domain.

The measurement results above also act as the fundamental basis on which inverter impedance emulation is built on. The frequency responses in Fig. 4.2 represent the innermost dynamics of the emulated inverter.

### 4.3.2 Stability of Emulated Inverter

To facilitate testing of impedance measurement algorithms, a three-phase inverter was emulated using the voltage amplifier, AC filter and real-time simulator. The test setup is as shown in 4.3. A three-phase inductor is connected between the two amplifiers, which are both operated in voltage-control mode. I.e., their internal controllers regulate their terminal voltages. The inductor serves two purposes. The first and most evident purpose is to provide impedance between the two voltage sources which are effectively connected in parallel. Without the impedance, it is very likely that the setup would either trip the protection circuits or damage to hardware would be caused. The second purpose of the inductor is to emulate the output filter of a grid-connected inverter and to facilitate suitable dynamic behaviour to allow emulating the fast AC current control loops.

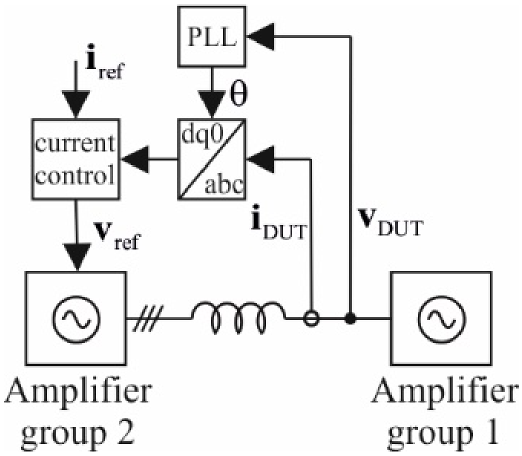


Figure 4.3: Test setup to evaluate stability of the emulated three-phase inverter.

The frequency responses measured previously are used to develop the open-loop dynamic model on top of which the current control loops are designed. Figure 4.4 shows the designed current control loops of the d and q-components of output current, which are extracted using the FRA. Moreover, Fig. 4.5. shows the designed and measured phase-locked-loop which is required to synchronize the current control with the AC voltage.

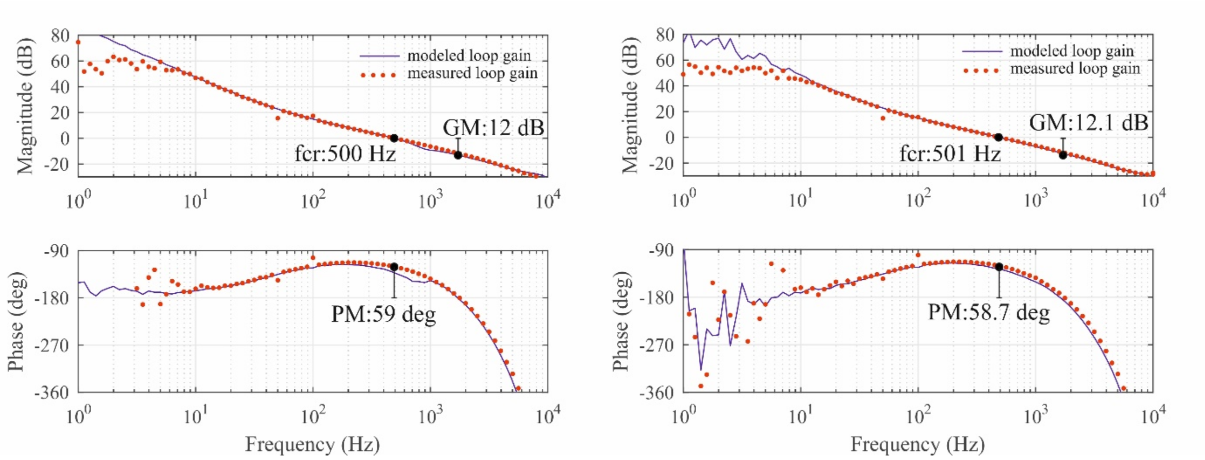


Figure 4.4: Designed and verified loop gains using the FRA.

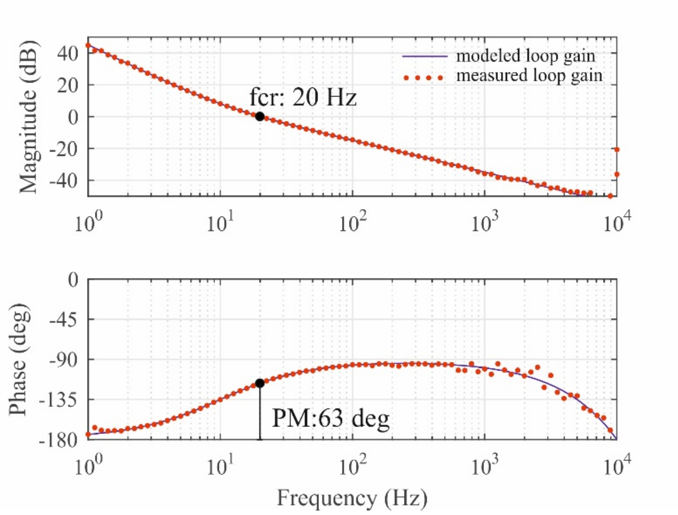


Figure 4.5: Designed and measured phase-locked-loop.

Figure 4.6 shows the waveforms of output current and output voltage when the grid voltage is subjected to a sudden symmetrical voltage dip of 25 percent. The current control reacts very fast and there seems to be no problem with the interaction of the internal voltage controls of the two amplifiers. Thus, the amplifier emulates the electrical behaviour of a real inverter very well in time-domain.

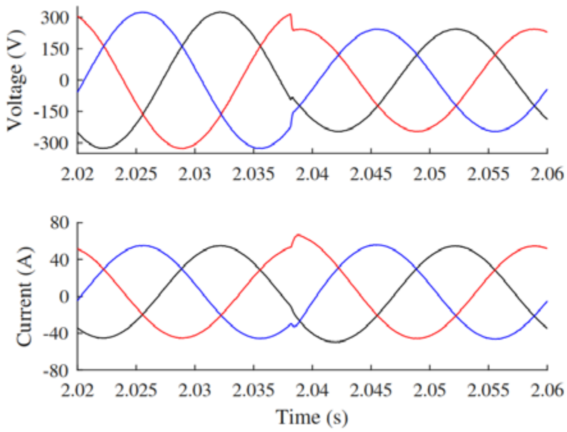


Figure 4.6: Step response of grid current when grid voltage experiences a 25 percent symmetrical dip.

Figure 4.7 shows a step response of the output current measured in the synchronous reference frame when the reference value of the current d-component was increased from 10 to 50 amps. The designed control system works as intended and there is little overshoot and settling time is just few milliseconds. Moreover, the lower waveform shows the step response when the crossover frequency of current control loop is intentionally reduced to 200 Hz and phase margin is only 35 degrees. Large oscillation is observed and the settling time is much longer. Thus, the system can represent similar time-domain behaviour as an inverter with insufficient stability margins and poor control design. Therefore, the setup can reveal insufficient control design even without measuring the actual control loop gains.

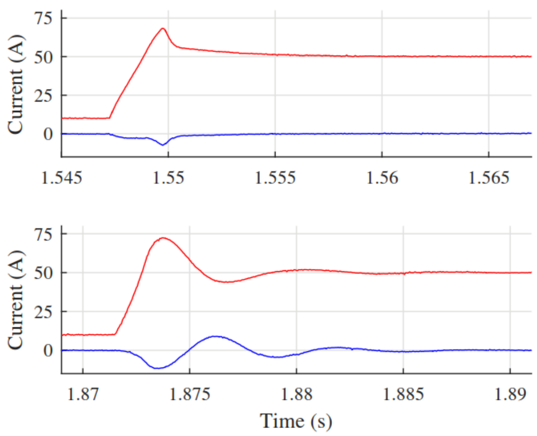


Figure 4.7: Step response of current in dq-domain with properly tuned current control (upper) and poorly tuned control system (lower).

It can be concluded that the voltage amplifier can be configured to resemble the dynamic behaviour of real grid-connected inverter. The time-domain response is directly linked to the tuning of current control loops as would be expected from actual inverter. Thus, the next step is to verify if the output impedance of the amplifier resembles that of a real inverter, i.e., to verify if the setup resembles a real inverter also in frequency-domain.

### 4.3.3 Impedance Measurement (Sine-Sweep)

To measure the emulated inverter impedance, a small-signal perturbation was added on top of the grid voltages. To be precise, the measured quantity is admittance, since the inverter is operated as a current source and grid voltage is an input variable. The admittance was measured by using a sine-sweep frequency response analyzer and PRBS injection method. Figures 4.8 and 4.9 show the measured admittance and the admittance given by an analytical model. The analytical model has been verified in previous research and it gives a good estimation for the real admittance [14]. Thus, it can be used as a reference to evaluate how well the inverter admittance can be emulated using the proposed setup.

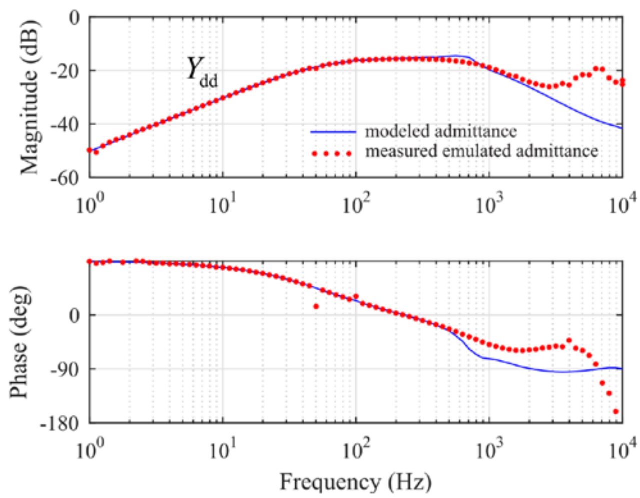


Figure 4.8: Measured emulated admittance (d-component) versus the modeled admittance of a real inverter.

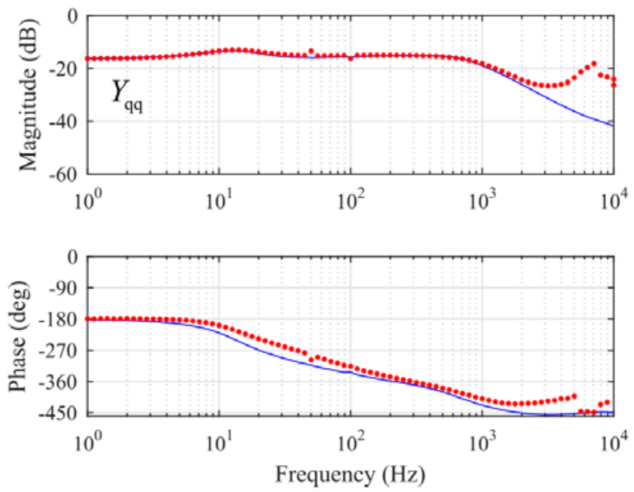


Figure 4.9: Measured emulated admittance (q-component) versus the modeled admittance of a real inverter.

It can be noticed that the emulated admittance d-component follows the reference up to approximately 500 Hz. It is no coincidence that this is the same frequency which was selected as the crossover frequency for the outer current control loop. Thus, after 500 Hz the internal voltage control of the amplifier starts to “fight back”, which prevents the passive properties of the L-filter from showing toward the grid. The admittance q-component follows its reference slightly higher, up to roughly 1 kHz.

### 4.3.4 PRBS method

The results above were extracted using the sine-sweep frequency response analyzer. Figurea 4.10 and 4.11 shows the results obtained by using the PBRS-method. The PRBS method gives exactly the same result as the sine-sweep method up to approximately 1 kHz. The bandwidth of the measurement could be increased by changing the PRBS parameters, such as generation and smapling frequency. However, it should be noted that the experimented PRBS measurement took around 5 seconds to measure the whole admittance matrix (4 components). Obtaining the same results with the FRA took about half an hour. Thus, it is much more efficient to use the PRBS method when the measurements are time critical or the operation is studied with many changing parameters.

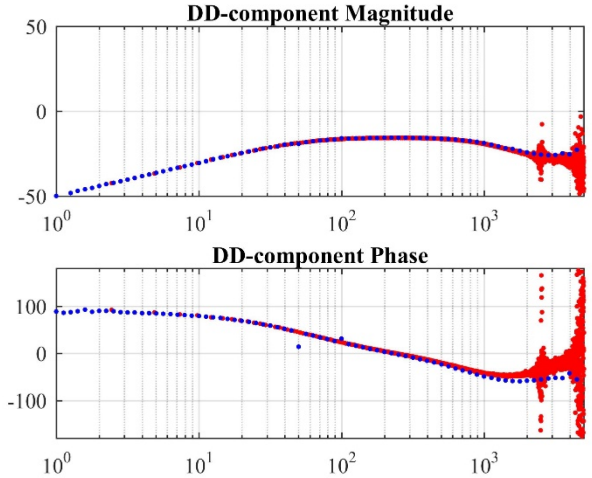


Figure 4.10: Measured admittance d-component using the FRA (blue) and the PRBS method (red).

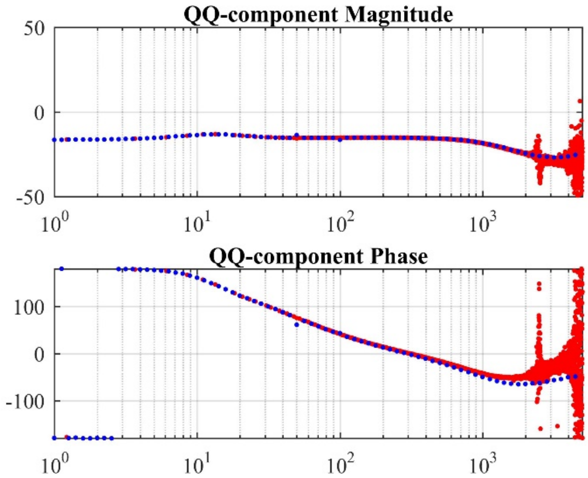


Figure 4.11: Measured admittance q-component using the FRA (blue) and the PRBS method (red).

## 4.4 Data Management and Processing

Data will be stored in TUTCRIS for later access, which is an online platform of Tampere University of Technology.

## 5 Results and Conclusions

The voltage amplifier was successfully used to reproduce the small-signal impedance behaviour, which is characterized by internal control loops. The effect of AC current control, phase-locked-loop and grid voltage feedforward on the impedance was evaluated. It was concluded that the impedance can be precisely emulated with correct magnitude and phase behaviour up until the bandwidth of the inner current control loop. The limiting factor at high frequencies was deemed to be the internal voltage control of the voltage amplifier, which was used to emulate the inverter power stage behaviour. The internal voltage control effectively hides the properties of the passive AC L-filter. However, this was considered acceptable since the internal voltage control guarantees relatively high safety and still the impedance-based interactions arising from all the control functionalities inside the AC current control bandwidth can be accurately emulated. However, the impedance measurement with FRA could easily capture the impedance up to 10 kHz which is more than enough to characterize high power converters. Moreover, by using the PRBS the measurement time is drastically reduced which is important if the effect of several parameters on impedance behaviour is to be studied.

### Open Issues and Suggestions for Improvements

It was observed that some amount of DC current flows between the amplifiers. This is caused by the fact that the converters operate internally in voltages control mode and there is no regulation for zero sequence current implemented on the real-time simulator. Thus, the small resistance of the inductance and cables and small deviation in the DC-levels of the two amplifier groups can cause significant DC current flowing in the circuit. This is a matter that needs to be taken into account in later setups, especially when the amplifier is connected to the actual grid or grid simulator.

The emulated impedance contains the effect of AC-side control loops. However, in theory it would be possible to simulate the DC side of the inverter using the real-time simulator to see the effect of of, e.g., DC voltage control loop on the emulated admittance.

The amplifiers are limited to 400 V, at least at the time of visit. Therefore, the voltage level is not enough to measure central inverters with 690 V AC nominal voltage.

Issues arising from the connection of grid simulator have not yet been identified.

## 6 Dissemination Planning

*Journal article in IEEE Transactions on Industrial Electronics*

One article has been submitted to a Special Section “On-board Micro-grids for the Electric Aircraft” which will be published by IEEE Transactions on Industrial Electronics. The article will discuss different identification techniques, such as maximum-length binary sequence, ternary sequence and orthogonal sequences, and specifically, their use in power electronics-based microgrids. The identified control loops and impedances from the Flex Power Grid Lab will be reported in the paper, along with discussion how the identification techniques can be implemented in power-electronics based power systems.

*Journal article in IEEE Transactions on Power Electronics*

Second journal article is under preparation to be submitted to IEEE Transactions on Power Electronics. The paper will discuss how a voltage amplifier can be configured to emulate the impedance behaviour or a real grid-connected three-phase inverter, by using a real-time simulator and AC filter. The paper presents the implementation, development of impedance model and various measured impedances obtained from the Flex Power Grid Lab. Moreover, the paper will discuss the potential limitations and risks involved with such impedance emulation.

*Journal article in Energies (open-access)*

Third journal article is also under preparation and will be submitted to open-access journal Energies. The article will show how the converter impedance changes between different operating modes and set points, e.g., inverter/rectifier mode, real/reactive power injection. The paper will make use of roughly 100 impedance curves measured during the visit at Flex Power Grid Lab. The paper will provide an extensive review based on the measured impedances.

# 7 References


[1] C. Li, “Unstable Operation of Photovoltaic Inverter from Field Experiences,” IEEE Trans. Power Deliv., vol. 8977, no. c, pp. 1–1, 2017.

[2] P. Belkin, “Event of 10/22/09,” CREZ Tech. Conf. Electr. Reliab. Counc. Texas, 2010.

[3] E. Mollerstedt and B. Bernhardsson, “Out of control because of harmonics-an analysis of the harmonic response of an inverter locomotive,” IEEE Control Syst., vol. 20, no. 4, pp. 70–81, Aug. 2000.

[4] L. Jessen and F. W. Fuchs, “Modeling of inverter output impedance for stability analysis in combination with measured grid impedances,” in 2015 IEEE 6th International Symposium on Power Electronics for Distributed Generation Systems (PEDG), 2015, pp. 1–7.

[5] J. H. R. Enslin and P. J. M. Heskes, “Harmonic interaction between a large number of distributed power inverters and the distribution network,” IEEE Trans. Power Electron., vol. 19, no. 6, pp. 1586–1593, 2004.

[6] P. C. Kotsampopoulos, F. Lehfuss, G. F. Lauss, B. Bletterie, and N. D. Hatziargyriou, “The Limitations of Digital Simulation and the Advantages of PHIL Testing in Studying Distributed Generation Provision of Ancillary Services,” IEEE Trans. Ind. Electron., vol. 62, no. 9, pp. 5502–5515, Sep. 2015.

[7] M. Cespedes and Jian Sun, “Impedance Modeling and Analysis of Grid-Connected Voltage-Source Converters,” IEEE Trans. Power Electron., vol. 29, no. 3, pp. 1254–1261, Mar. 2014.

[8] L. Harnefors, X. Wang, A. Yepes, and F. Blaabjerg, “Passivity-Based Stability Assessment of Grid-Connected VSCs - An Overview,” IEEE J. Emerg. Sel. Top. Power Electron., vol. 4, no. 1, pp. 116–125, 2015.

[9] Ł. H. Kocewiak, C. Álvarez, P. Muszynski, J. Cassoli, L. Shuai, “Wind Turbine Harmonic Model and Its Application – Overview, Status and Outline of the New IEC Technical Report,” in Proc. The 14th International Workshop on Large-Scale Integration of Wind Power into Power Systems as well as Transmission Networks for Offshore Wind Farms, 2015.

[10] A. Aapro; T. Messo; T. Roinila; T. Suntio, "Effect of Active Damping on Output Impedance of Three-Phase Grid-Connected Converter," in IEEE Transactions on Industrial Electronics , vol.PP, no.99, pp.1-1

[11] T. Roinila, T. Messo and A. Aapro, “Impedance measurement of three-phase systems in DQ-domain: applying MIMO-identification techniques”, IEEE Energy Conversion Congress and Exposition, Milwaukee, Wisconsin, U.S., pp. 1-6, 2016.

[12] T. Messo, A. Aapro, T. Suntio and T. Roinila, “Design of grid-voltage feedforward to increase impedance of grid-connected three-phase inverters with LCL-filter”, 2016 IEEE 8th International Power Electronics and Motion Control Conference (IPEMC-ECCE Asia), Hefei, pp. 2675-2682, 2016.

[13] M. Jaksic, Z. Shen, I. Cvetkovic, D. Boroyevich, R. Burgos, C. DiMarino, and F. Chen, “Medium-Voltage Impedance Measurement Unit for Assessing the System Stability of Electric Ships,” IEEE Trans. Energy Convers., vol. 8969, no. c, pp. 1–1, 2017.

[14] T. Suntio, T. Messo and J. Puukko, “Power Electronic Converters: Dynamics and Control in Conventional and Renewable Energy Applications”, Textbook, Wiley-VCH , 720 pages, 2017.